Comparative Actualistic Study Hints at Origins of Intriguing Miocene “Coprolites” of Poland

Tomasz Brachaniec
University of Silesia in Katowice
Dorota Środek
University of Silesia in Katowice
Dawid Surmik
University of Silesia in Katowice
Robert Niedźwiedzki
Wrocław University
Georgios L. Georgalis
University of Zurich
Bartosz J. Płachno
Jagiellonian University in Kraków
Piotr Duda
University of Silesia in Katowice
Alexander Lukeneder
Natural History Museum Vienna
Przemysław Gorzelak
Polish Academy of Sciences
Mariusz A. Salamon (paleo.crinoids@poczta.fm)
University of Silesia in Katowice

Research Article

Keywords: Intriguing Miocene , Coprolites, Poland

Posted Date: September 7th, 2021

DOI: https://doi.org/10.21203/rs.3.rs-864768/v1

Comparative actualistic study hints at origins of intriguing Miocene "coprolites" of Poland

Tomasz Brachaniec[1], Dorota Środek[1], Dawid Surmik[1], Robert Niedźwiedzki[2], Georgios L. Georgalis[3], Bartosz J. Płachno[4], Piotr Duda[5], Alexander Lukeneder[6], Przemysław Gorzelak[7], Mariusz A. Salamon[1*]

[1]University of Silesia in Katowice, Faculty of Natural Sciences, Będzińska 60, 41-200 Sosnowiec, Poland, paleo.crinoids@poczta.fm (MAS - corresponding author)
[2] Institute of Geological Sciences, Wrocław University, Borna 9, 50-204 Wrocław, Poland
[3]Palaeontological Institute and Museum, University of Zurich, Karl Schmid-Strasse 4, 8006 Zurich, Switzerland
[4]Jagiellonian University in Kraków, Faculty of Biology, Institute of Botany, Gronostajowa Street 9, 30-387 Cracow, Poland
[5]University of Silesia in Katowice, Faculty of Science and Technology, Będzińska Street 39, 41-200 Sosnowiec, Poland
[6]Natural History Museum Vienna, Burgring 7, 1010 Vienna, Austria
[7]Institute of Paleobiology, Polish Academy of Sciences, Twarda 51/55, 00-818 Warszawa, Poland

Abstract

Excrement-shaped siderite masses have been the subject of much controversy. They have been variously interpreted either as being coprolites, cololites or pseudofossils created by mechanical deformation of plastic sediment. Here we report excrement-shaped ferruginous masses recovered from the Miocene of the Turów mine in south-western Poland. Mineralogical, geochemical, petrographic and microtomographical analyses indicate that these masses consist of siderite and iron oxide rather than phosphate, and rarely contain recognizable food residues, which may suggest abiotic origins of these structures. On the other hand, evidence in support of a faecal origin include: (i) the presence of two distinct morphotypes differing in size and shape, (ii) the limited quantity of specimens, (iii) the presence of rare hair-like structures or coalified inclusions and (iv) the presence of fine striations on the surface. Importantly, comparative actualistic studies of Recent vertebrate feces show overall resemblance of the first morphotype (sausage-shaped with rare coalified debris) to excrements of testudinoid turtles (Testudinoidea), whose shell fragment was found in the investigated locality. The second morphotype (rounded to oval-shaped with hair-like structures), in turn, is similar to the feces of some snakes (Serpentes), the remains of which were noted in the Miocene of the neighborhood areas.

Introduction

Incontrovertible examples of the Miocene coprolites are known from only a few localities in Europe, North and South America[1-7]. Rodents, notoungulates, hathliacynid and borhyaenoid marsupials, indeterminate carnivorans, sirenians, and crocodilians were commonly invoked as potential producers of these coprolites[3,5-6]. The majority of described Miocene vertebrate coprolites were produced by carnivores. This is not surprising because faeces of herbivorous tetrapods are commonly composed of a large quantity of undigested plant residues attracting microbial decomposition. On the other hand, the calcium phosphate derived from undigested bones in the faeces of carnivores acts as important permineralizing agent[5,8-9].

Excrement-shaped ferruginous masses have been considered (based on morphological grounds) by some authors as being coprolites or cololites (intestinal casts)[10-11]. These objects are commonly reported from clay-rich sediments ranging in age from Permian to Holocene. However, given their ferruginous composition, significant variation in size, lack of internal inclusions, and scarcity of associated vertebrate remains, most authors rejected the coprolite nature[12-24]. Different hypotheses have been invoked to explain the origins of these objects (such as soft sediment extrusion triggered by coseismic liquefaction, sediment intrusion into hollow logs, expulsion of sediment in response to gravity, extrusion of siderite related to methanogenesis).

Until recently, a detailed study on excrement-shaped ferruginous masses from the Miocene of Poland has been lacking. In this paper we analyse the Miocene excrement-shaped specimens collected from the coal mine of Turów for the first time. According to our results, we favour the hypothesis that the specimens from Poland represent true coprolites and more particularly pertaining to two different reptile groups.

Geological setting

The Turów lignite mine is located in the south-eastern part of the Lower Silesia Voivodeship (SW Poland) and covers the former village of Turów. It is located in the central part of the mesoregion Żytawa-Zgorzelec Depression located between the state borders of Germany and the Czech Republic (Fig. 1A). Turów lignite deposits are part of the Upper Lusatian Brown Coal Basin. This basin comprises a few tectonic sinkholes[25] that developed in Paleogene at the junction of two regional zones of strong activity: Ore Mts. Graben (Ohrza rift) and the Lusatian-Elbe Tectono-Volcanic Zone[26]. The most southern of these[25] is the Zittau Basin (Fig. 1A, B), which was filledmainly by limno-fluvial or limnic clays, silts, sands and thick layers of lignites exploited in the Turów mine[27-28]. Furthermore, there are numerous volcanic rocks of late Eocene, Oligocene and early Miocene age[28]. The basal part of sedimentary section of the Zittau basin is not older than the early Oligocene, however most sediments were formed in the Miocene[28]. At the base of the Zittau Basin, Precambrian and Palaeozoic metamorphic and igneous rocks are present[29].

The lithological profile of the Turów mine is ca. 250 m thick and consists of 7 lithostratigraphic units of sedimentary rocks. Apart from the two youngest units (Gozdnica Fm. and glacial tills), all of them are mainly composed of clays and/or muds. Additionally, there are coal seams, especially in Opolno and Biedrzychowice formations, which are the deposits mined at the Turów mine. The oldest Cenozoic sediments of the profile are Oligocene sediments (Egger age), forming the lower part of the Turoszów Fm.[28]. The youngest in the profile are gravels and sands of the Gozdnica Fm. Pannonian in age and Pleistocene deposits, mainly represented by tills[30].

The Turoszów Fm. was formed in fluvial and limnofluvial conditions, while the Opolno and Biedrzychowice Fms have been formed in limnotelmatic environments, and Porajów Fm. represents limnofluvial environment. Sediments of the upper part of Miocene profile (Rybarzowice and Gozdnica Fms.) have alluvial origin[31]. Biedrzychowice Fm., within which excrement-shaped ferruginous masses and a turtle remain have been documented, was formed in vast swamps and rushmarshes[32]. Especially in the upper part of this formation, there are numerous palaeosols levels with plant roots and trunks preserved in situ[33]. Marsh forests mainly composed of *Cupressaceae* and *Taxaceae*[33-34]. Based on palaeobotanical analysis of the coal seam it was concluded that there was a humid warm temperate climate similar to that of south-eastern China today[32,35].

The ferruginous masses and the turtle shell fragment documented in this article were collected in an inactive part of the excavation, within the clays of the higher part of Biedrzychowice

Fm. in the uppermost part of early Miocene (Burdigalian; see Fig. 1C). Two distinct morphotypes randomly distributed within clay on the flat surface of the excavation were noted.

Figure 1 around here

Fossil content in the Turów area and adjacent areas

No animal fossil remains have been documented so far from the Oligocene–Miocene of the Zittau Basin with exception of burrows of sediment eating fauna[28]. In the course of the present research in the clays of Biedrzychowice Fm., apart from the excrement-shaped ferruginous masses, a fragment of a turtle shell was found. This shell fragment (Fig. 2N) can only be identified as an indeterminate testudinoid. This turtle lineage is otherwise abundant in Oligocene and early Miocene localities in Germany and Czech Republic[37-38] but had not so far been documented from coeval localities in Poland. In older, Eocene and Oligocene localities in the neighbouring north-western Czech Republic and south-eastern Germany (Saxony and southeastern Saxony-Anhalt), rich assemblages of terrestrial-aquatic tetrapod fauna have been documented, comprising frogs, salamanders, choristoderans, crocodiles (also crocodile coprolites, see[28] and literature cited therein), turtles, lizards, and snakes (Table 1).

Table 1. Oligocene vertebrates (amphibians and reptiles) collected in adjacent areas (north-western Czech Republic and south-eastern Germany [Saxony, south-eastern Saxony-Anhalt]); after [39-57].

Age	Locality	Amphibians	Reptiles
late Oligocene	Lužice-Žichov (Czech Republic)	*Triturus opalinus* *Rana luschitzana* *Asphaerion reussi*	
	Suletice (Czech Republic)	*Archaeotriton basalticus* *Palaeobatrachus grandipes* *Palaeobatrachus laubei*	
	Bechlejovice (Czech Republic)	*Archaeotriton basalticus* *Palaeobatrachus diluvianus* *Palaeobatrachus luedeckei* *Palaeobatrachus robustus* *Palaeobatrachus grandipes* *Palaeobatrachus novotnyi* *Eopelobates bayeri*	*'Diplocynodon'* sp.
early Oligocene	Espenhain, Saxony (Germany)		Trionychidae indet. *Pelorochelon* sp. *Diplocynodon* sp.
	Kundratice (Czech Republic)	*Palaeobatrachus* sp. cf. *Eopelobates* sp.	cf. *Diplocynodon* sp.
	Lukavice (Czech Republic)		*'Diplocynodon'* sp.
	Markvartice (Czech Republic)	*Chelotriton laticeps* *Palaeobatrachus diluvianus* *Palaeobatrachus luedeckei* *Palaeobatrachus* sp.	
	Dětaň (Czech Republic)	Salamandridae indet. Palaeobatrachidae indet. Pelobatidae indet. Discoglossidae indet.	Lacertidae indet. Anguidae indet. Testudinidae indet.

			Serpentes indet. Crocodylia indet.

On the other hand, in the lower Miocene clays and sands of North Bohemian Brown Coal Basin, a very rich fauna assemblage was reported[2]. The latter mentioned and illustrated numerous invertebrates and vertebrates represented by osteichthyan fishes, amphibians, reptiles, birds, and mammals. The reptile taxa are shown in the table below (Table 2).

Table 2. Reptiles recorded in the lower Miocene deposits of North Bohemia, Czech Republic (taken from[2,38,57-70]).

turtles	**crocodiles**	**lizards**	**snakes**	**Choristoderans**
			Scolecophidia indet.	
			Bavarioboa hermi	
	Diplocynodon cf. *ratelii*	*Merkurosaurus ornatus*	*Bavarioboa* sp.	*Lazarussuchus dvoraki*
			Constrictores indet.	
			Falseryx petersbuchi	
		Pseudopus ahnikoviensis	"*Coluber*" *dolnicensis*	
		Pseudopus confertus	*Texasophis bohemiacus*	
		Pseudopus sp.		
		Ophisaurus fejfari		
Rafetus bohemicus		*Ophisaurus holeci*	"*Coluber*" *suevicus*	
		Ophisaurus robustus		
		Ophisaurus spinari		
		Ophisaurus aff. *spinari*		
		Ophisaurus sp. (two morphotypes)		
		Anguinae indet. (several morphotypes)		
		Palaeocordylus bohemicus		
Trionychinae indet.		aff. *Palaeocordylus bohemicus*	"*Coluber*" *caspioides*	
			"Colubrinae" indet.	
Ptychogaster laubei		*Euleptes gallica*	*Elaphe* sp.	
Ptychogaster cf. *emydoides*		*Chamaeleo andrusovi*		
Ptychogaster sp.		Chamaeleonidae indet.	*Natrix sansaniensis*	
		Amblyolacerta dolnicensis		
Chelydropsis sp.		*Lacerta* sp.	*Natrix merkurensis*	
		Miolacerta tenuis	*Neonatrix nova*	
		Lacertidae indet.	*Palaeonatrix lehmani*	
		cf. Scincidae indet.		
		Blanus gracilis	Natricinae indet.	
		Squamata indet.	Elapidae indet.	
			Macrovipera platyspondyla	
			Vipera antiqua	

Testudinidae indet.			*Vipera* sp.	
			Viperidae indet.	

Results

"Coprolite" morphotypes

29 specimens of excrement-shaped ferruginous masses were collected. Among these specimens two different shapes and sizes were identified. More specifically, morphotype 1 (M1) is represented by small (up to 40 mm long, see Table 3) sausage-shaped specimens with smooth or rough surface and flared lower part (Fig. 2A, B; compare Fig. 2C, D). Morphotype 2 (M2), in turn, is represented by large (up to 63 mm long) and more rounded to oval, massive specimens with rough surface (Fig. 2E-G; comare Fig. 2H-K). Some specimens (Fig. 2F, G) included into M2, bear prominent pointed end covered by striate pattern (herein interpreted as a trace produced after closing anus, see Discussion below). Color of both morphotypes varies from pale orange, through greenish red, to burgundy-colored.

Figure 2 around here

Table 3. Summary for excrement-shaped ferruginous masses.

specimen no.	morphotype	dimensions (diameter at its narrowest point*diameter at its widest point*lenght); all are given in mm	inferred producer
GIUS 10-3739/1	M1 (see Fig. 2B, C)	7*14*32	Testudinoidea
GIUS 10-3739/2	M1 (see Fig. 2A)	9*20*44	Testudinoidea
GIUS 10-3739/3	M1	9*18*30	Testudinoidea
GIUS 10-3739/4	M1	6*17*31	Testudinoidea
GIUS 10-3739/5	M1	10*17*34	Testudinoidea
GIUS 10-3739/6	M1	11*19*34	Testudinoidea
GIUS 10-3739/7	M1	8*15*29	Testudinoidea
GIUS 10-3739/8	M2 (see Fig. 2F)	45*63*41	Serpentes
GIUS 10-3739/9	M2 (see Fig. 2G)	31*48*37	Serpentes
GIUS 10-3739/10	M2 (see Fig. 2I, J)	8*34*34	Serpentes
GIUS 10-3739/11	M2 (see Fig. 2K)	25*54*38	Serpentes
GIUS 10-3739/12	M2 (see Fig. 2M)	20*41*27	Serpentes
GIUS 10-3739/13	M2	31*44*35	Serpentes
GIUS 10-3739/14	M2	41*60*51	Serpentes
GIUS 10-3739/15	M2	34*56*51	Serpentes
GIUS 10-3739/16	M2	27*49*38	Serpentes
GIUS 10-3739/17	M2	32*54*53	Serpentes
GIUS 10-3739/18	M2	32*36*29	Serpentes
GIUS 10-3739/19	M2	21*42*61	Serpentes
GIUS 10-3739/20	M2	20*44*39	Serpentes

GIUS 10-3739/21	M2	26*58*36	Serpentes
GIUS 10-3739/22	M2	25*56*28	Serpentes
GIUS 10-3739/23	M2	33*48*39	Serpentes
GIUS 10-3739/24	M2	21*26*33	Serpentes
GIUS 10-3739/25	M2	24*34*35	Serpentes
GIUS 10-3739/26	M2	31*40*39	Serpentes
GIUS 10-3739/27	M2	16*32*29	Serpentes
GIUS 10-3739/28	M2	30*42*35	Serpentes
GIUS 10-3739/29	M2	18*30*29	Serpentes

Thin sections made from specimens no. GIUS 10-3739/28, 29 are acronymed GIUS 10-3739/TS.

Optical microscopy, microtomographic and palaeontological studies

The thin sections from two specimens representing two morphotypes were studied both under transmitted and reflected light optical microscopy. The sections from both morphotypes look very similar. They are dominated by darker matrix almost not translucent making transmitting light observations difficult. The mineral matrix seems to be rather homogenous. Within the matrix of M2-type more translucent elongated straight or curly structures (up to about few mm long and 10-99 µm thick; mean: 52 µm) are visible (Fig. 3). The structures sometimes form arcs or are twisted. In the reflected light, they seem to be areas of light reduction, while surrounding matrix is oxidized. The dark (rusty-colored, brown to almost black), poorly translucent coloring of a matrix suggests iron-rich mineral which form the matrix. Therefore both mineral matrix as well as thin elongated straight to curly structures were studied in-depth under SEM and Raman imaging (see below). No other distinguishable microremains were noticed in thin sections. However, at the broken surfaces of some specimens of the first morphotype (M1) some tiny coalified debris were occasionally noticed (Fig. 2A, B).

Figure 3 around here

Microtomographical studies of selected specimen (GIUS 10-3739/23; Supplementary Movie 1) did not reveal any internal structures, which could have been eventually interpreted as undigested food remains.

Mineralogical, geochemical and structural analyses

XRD analyses of powdered fragments of two specimens from each morphotypes indicated that both are composed of siderite with small admixture of geothite, and hematite (Supplementary Figure 1).
The more detailed data on microstructure and elemental composition were collected by utilizing SEM/EDS. We found that the matrix is composed of irregular forms organized in net-system structures (Fig. 4). These forms are bound by thin walls that often consist of several layers (Fig. 4G, H). The chemical analyses showed that the walls consist of iron oxides and the interior is likely filled with iron carbonate. Two types of matrix occurring in both morphotypes (M1 and M2) were distinguished. The first one includes smaller (up to 10 µm in diameter) forms with a broad wall of iron oxides and an empty inner part (Fig. 4A-F). Occasionally, larger forms with carbonate centers (up to 100 µm in diameter) can also be found in the vicinity of the large voids (Fig. 4G). Due to the presence of unfilled forms in the

matrix, a distinct porosity pattern can be visible (Fig. 4A1-F1). In this matrix type, within specimen of M2-type straight or curly elongated structures, which were also observed under optical microscopy, can be found (Fig. 3, 4A-F). They can occur as thin (10-99 µm) lines with significantly limited porosity (Fig. 3, 4A-B1, C-F1). In the widest cross sections, some cellular structure is observed (Fig. 3H, 4A-B1), while in the narrowest cross sections (Fig. 4C-F1), characteristic scale-like pattern in observed (Fig. 3F, G, 4C-F1). The second type of matrix consists of larger (up to 30 µm in diameter) forms characterized by thinner walls (Fig. 4I, J). Their center is always filled with iron carbonate, so there is no distinct porosity, as well as no elongated structures to be found.

Figure 4 around here

To extend the observations and elemental analysis based on SEM, Raman spectra were collected. The data obtained from Raman spectroscopy allows to differentiate two iron oxides within the walls (Fig. 5A, B). The spectrum of the first one has bands at 1322, 662, 407, 296, and 227 cm^{-1} (Fig. 5A), which are characteristic for the hematite[71]. The second mineral forms only very thin (<1 µm) layers in the hematite. The main bands of its spectrum are 684, 553, 397, 299, and 242 cm^{-1} (Fig. 5B), which allow identifying this mineral as goethite[71]. The 1322 cm^{-1} band at the goethite spectrum originated from the admixture of the hematite. The spectrum of the carbonate mineral contains bands connected to the typical vibrations of the CO_3 group (Fig. 5C), and it can be recognized as siderite[72].

Figure 5 around here

The Raman spectroscopy was also used to investigate the thin elongated structures in the matrix. There was no variation in the mineralogical composition of these forms in comparison to the matrix. However, during experiments with the 532 nm laser (green), we observed increased fluorescence in the area of the elongated structures with reduced porosity (Fig. 6). This may indicate that although these structures are composed of the same minerals as the matrix, their original chemical composition was different.

Figure 6 around here

Comparative actualistic studies

For comparative purposes we investigated modern faeces (789 in total) produced by a number of vertebrates, comprising all major groups (i.e., fish, amphibians, reptiles, birds, and mammals) (for details see Supplementary Tables 1-4). We noticed that our excrement-shaped ferruginous masses ascribed to the morphotype 1 are very similar to sausage-shaped excrements produced by two testudinid turtle taxa [i.e., the Mediterranean tortoise (*Testudo hermanni*) and the steppe tortoise (*Testudo horsfieldii*)]. Their surfaces are mainly smooth and rarely covered with cracks (e.g., Fig. 3C, D); the digested plant debris are sometimes visible on their surfaces (Fig. 3C, D). We also compared the fossil excrements with excrements of other extant turtles [another testudinid, i.e., the Indian star tortoise (*Geochelone elegans*), a geoemydid, i.e., the Spanish pond turtle (*Mauremys leprosa*), and a trionychid, i.e., the Nile softshell turtle (*Trionyx triunguis*)], but the feaces of the *Trionyx triunguis* differ in size and shape. On the other hand, our excrement-shaped ferruginous masses ascribed to the morphotype 2 are very similar to more or less rounded to oval, massive excrements produced by three snake taxa [the king python (*Python regius*), the common boa (*Boa constrictor*), and the king cobra (*Ophiophagus hannah*)]. Their surfaces are rough, and often contain some

remnants of etched hair and feathers (e.g., Fig. 3H). Moreover, the faeces of the Korean rat snake (*Elaphe anomala*) are also similar to the fossil morphotype 1; however, they differ in size (they are smaller). The excrement surfaces of the latter species are covered by some hairs. We also observed three excrements of the common European viper (*Vipera berus*). They are different in shape and size one from another, their surfaces are covered by etched hair (Fig. 2L, M).

Discussion

Although in the Biedrzychowice Fm. there are numerous inorganic siliceous and siderite concretions ([32], personal observations), they have a different external morphology (i.e., they do not reveal a characteristic excrement-like shape) and internal structure (i.e., they typically have a concentric zoning). On the one hand, results of our geochemical, mineralogical, petrographic and microtomographical analyses indicate that excrement-shaped masses from Turów mainly consist of siderite and iron oxide rather than phosphate, and rarely contain recognizable food residues, which may indicate abiotic origins of these structures. However, evidence in support of a fecal origin include: (i) the presence of two distinct morphotypes differing in size and shape, (ii) the limited quantity of specimens, (iii) the presence of fine striations on the surface, and (iv) the presence of hair-like elongated structures or coalified inclusions.

Spencer[21] argued that parallel striations in the pseudocoprolites from the Miocene of southwestern Washington State might have resulted from passage of the material over the grain of the wood. However, in the case of the specimens from Poland, parallel striations, which are observed in a few specimens, are more reminiscent of marks left by the anal sphincter because these marks are not randomly distributed but are located in the pointed end of the specimens (Fig. 3F, G).

Although mineralogy of the excrement-shaped masses from Poland is not indicative of coprolites, it might have been a result of diagenesis. Indeed, Seilacher et al.[11] noted that similar excrement-shaped ferruginous masses from the Miocene of southwestern Washington State might have been alternated by secondary processes referred to as the ‘‘roll-fronts’’ of oxidized groundwater[73-74], which dissolves calcite and phosphates bones and precipitates ferroan carbonates. The presence of numerous voids and lack of clay minerals within excrement-shaped ferruginous masses from Poland is consistent with this scenario. Furthermore, lack of phosphates in the coprolites may be additionally explained by the fact that they were produced by predominantly herbivorous animals[75-77]. Notably, within the morphotype 1 some tiny coalified debris were noted. The morphotype 2, in turn, contains only some elongated thin structures, which are reminiscent of hairs. Their mean size (52 μm) falls well within the range of the hair diameter (14-160 μm) of extant animals [78-79]. Furthermore, their morphologies, i.e., some cellular structure observed in the widest longitudinal sections (Fig. 2H, 4A-B1) and characteristic scale-like pattern observed in the narrowest longitudinal sections (Fig. 4C-F1), are similar to the inner cellular structure of medulla and outer scale-like layers of the extant and fossil hairs[80]. If these excrement-shaped masses indeed represent true coprolites, this may indicate that the digestive system of the producer was highly efficient, i.e., it dissolved and absorbed everything but the prey's hair, which were excreted along with faeces.

The presence of two distinct morphotypes, differing in size and shape suggests that they might have been expelled from the two different producers. Indeed, comparative actualistic study of Recent vertebrate faeces shows overall resemblance of the first morphotype (sausage-shaped with rare coalified debris) to excrements of turtles of the group Testudinoidea. This is further supported by the fact that a testudinoid shell fragment was also recovered in the Turów mine,

that being also the sole so far found vertebrate fossil from that locality. Within Testudinoidea, tortoises (Testudinidae) are terrestrial, while the other two groups that inhabited and still inhabit Europe (Emydidae and Geoemydidae) are aquatic or at least semiaquatic. Testudinoids have been already known in the Polish fossil record, however, their earliest occurrence so far was documented in younger strata, i.e., the middle Miocene (MN 6) locality of Nowa Wieś Królewska near Opole [81]. That being said, the single shell fragment from Turów represents the earliest testudinoid occurrence from Poland. Nevertheless, testudinoids are already known from early Miocene localities in the vicinity area of northwestern Czech Republic and southeastern Germany (see Table 2). Other turtle lineages, such as chelydrids and trionychids are found in the same vicinity area – among them, the former group is also found in the middle Miocene of Poland[68], while the latter has never been so far identified from that country [57].

On the other hand, the second coprolite morphotype from the Turów mine (morphotype M2) approaches more in its overall morphology the excrements of extant species of snakes. More particularly, there is a high degree of resemblance with large snake species of Constrictores (*sensu*[82]; i.e., booids and pythonoids). Nevertheless, an overall resemblance of M2 is also apparent with excrements of large caenophidians, such as the elapid *Ophiophagus* and the colubrid *Elaphe*, while, conversely, smaller caenophidian taxa, such as the viperid *Vipera berus* and the colubrid *Pantherophis*, seem to produce very differently-shaped excrements, which are relatively thin and tightly curled. As such, it is probable that the excrement shape within snake taxa could be somehow size-constrained and does not have a clear taxonomic/phylogenetic value as per its exact affinities. In addition, lizards can be excluded as possible candidate producers for morphotype M2, as excrements of extant large lizard taxa, such as anguids and varanids (which have also an abundant fossil record in the early Miocene of Central Europe) were much differently-shaped. This being said, on the absence of any accompanying skeletal fossil specimen from Turów, we can only infer that the coprolite morphotype M2 was produced by large, but still indeterminate, snakes. Afterall, large snakes were rather abundant in the Burdigalian of Central Europe, being also rather diverse, pertaining to a number of different lineages (Booidea, Pythonoidea, Colubridae, Natricidae, Elapidae, Viperidae) (see Table 2). It is noteworthy that snakes are known to maintain of a very acidic pH during digestion and dissolve and absorb everything but the prey's hair (or feathers) and claws, which are excreted along with waste[83-84].

Conclusions

The excrement-shaped ferruginous masses and the turtle shell fragment from the early Miocene of Turów mine in Poland have been described for the first time. Although different hypotheses were invoked to explain the origins of similar excrement-shaped ferruginous masses, we favour the hypothesis that at least the specimens from Poland represent true coprolites. Evidence in support of a faecal origin of these structures include the presence of two distinct morphotypes differing in size and shape, the limited quantity of specimens, the presence of hair-like structures or coalified inclusions, and the presence of fine striations on the surface. We suggest that the first morphotype (sausage-shaped with rare coalified debris) might have been produced by tortoises (Testudinoidea), whereas the second morphotype (rounded to oval-shaped with hair-like structures) likely represents fossil faeces of snakes (Serpentes).

Material and methods

Among 29 coprolites obtained from the investigated locality, 10 representative coprolites were selected for detailed investigation. A tortoise shell fragment, documented macroscopically in the field and found on a flat surface of upper part of the Biedrzychowice Fm., was also subjected to further observations. All specimens are housed in the Institute of Earth Sciences of the University of Silesia in Katowice, Poland, and catalogued under registration number GIUS 10-3739.
A clay sample weighing ca. 40 kg was also collected from Biedrzychowice Fm. and transported to the Laboratory of the Institute of Earth Sciences of the University of Silesia in Katowice. It was washed using running hot tap water, screened on a sieve column (Ø1.0, 0.315 and 0.1 mm-mesh respectively), and finally dried at 180˚C. This washed and dried residue was observed under a Leica Wild M10 microscope for vertebrate remains; unfortunately, nothing was found in the residue.
Coprolites recorded herein have been investigated with a number of different analytical tools.

Optical microscopy

Optical observation of thin sections were carried out using Leica SZ-630T dissecting microscope and Nikon Eclipse E100 light microscopy,while the microphotographs were collected using Olympus BX51 polarizing microscope equipped with an Olympus SC30 camera and a halogen light source, installed Faculty of Natural Sciences at the University of Silesia in Katowice (Poland).

Scanning Electron Microscopy

The chemical composition, morphology of coprolite matrix and microstructures topography were investigated using the desktop scanning electron microscopy (SEM) Phenom XL, PhenomWorld (ThermoFisher Scientific, Eindhoven, Netherlands) equipped with a fully integrated energy-dispersive X-ray spectroscopy (EDS) detector and secondary electron detector (SED) located in the Faculty of Natural Sciences at the University of Silesia in Katowice (Poland). Measurements were performed with low-vacuum settings with accelerating voltage 15 kV.

Microtomography

Virtual sections of a selected specimen (GIUS 10-3739/23) were made in the Faculty X-ray Microtomography Laboratory at Faculty of Computer Science and Material Science, University of Silesia in Katowice, Chorzów, Poland using the General Electric Phoenix v|tome|x micro-CT equipment at 160 kV, 70µA and scanning time of 20 min. Projection images were captured using a 1000 × 2024 pxs scintillator/CCD with an exposure time of 250 ms and processed using Volume Graphics® VGSTUDIO Max software and analysed using Volume Graphics® myVGL viewer.

Thin-sectioning

Thin sections from two specimens representing two morphotypes were made in the Grindery at the Faculty of Natural Sciences, University of Silesia in Katowice, Sosnowiec, Poland. Specimens were embedded in Araldite epoxy resin, sectioned, mounted on the microscope slides and polished with silicon carbide and aluminium oxide powders to about 30 µm thick.

Confocal Raman spectroscopy

To determine the mineralogical composition, the WITec confocal Raman microscope CRM alpha 300M equipped with an air-cooled solid state laser (λ = 532 nm and λ = 457 nm) and an electron multiplying CCD (EMCCD) detector was used. The calibration of the instrument was verified by checking the Si position. The Raman scattered light was focused onto a multi-mode fiber and monochromator with a 600 line/mm grating. To collect spectra of the coprolite matrix phases, the 50x/0.76NA and 100x/0.9NA air Olympus MPLAN objectives were used. All spectra were collected in the 200-4000 cm^{-1} range with 3 cm^{-1} spectral resolution. A surface Raman imaging map was collected in a 140 x 25 μm area using 140 x 20 pixels with an integration time of 0.5 s per spectrum, and precision of moving the sample during the measurements of ± 0.5 μm. The cluster analysis was performed to group spectra into clusters. K-means analysis with the Manhattan distance for Raman imaging maps was carried out. The data obtained was manipulated by WITec Project FIVE Software (cosmic rays removal procedure and cluster analysis) and GRAMS software package (baseline correction).

XRD

Bulk mineral composition of two powdered specimens representing each morphotypes was determined by Debye-Sherrer X-ray method using Rigaku SmartLab diffractometer equipped with Cu Kα1 source radiation. Measurement parameters were: acceleration voltage: 45 kV; filament current: 200 mA; step size: 0.05° 2Θ. Analyses of the collected data were carried out by means of XRAYAN Software using the newest ICSD database.

Observations of extant excrements

Faeces of Recent animals (private farms and from animals raised at the Silesian Zoological Garden in Chorzów, ZOO Wrocław, both in Poland) were observed. Over the course of two months, a total of 787 excrements belonging to modern fish, amphibians, reptiles, birds and mammals were collected. Lineages that had their representatives in the early Miocene sediments of North Bohemia, Czech Republic (see Supplementary Tables 1-4) were selected for a more detailed observation. Additionally, the animals had to be large enough to produce excrements with dimensions comparable to those currently documented in the fossil state. Thus, the faeces of small fish, the remains of which are known from the Miocene sediments of North Bohemia, such as *Chalcaburnus* or *Nemacheilus*, toads and frogs (*Rana*, *Pelobates*), birds (*Upupa*, *Coturnix*) and mammals (Chiroptera, *Dryomys*, *Sciurus*, *Martes*), were not taken into account.
Those that taxa that left their excrement in the aquatic environment were also rejected; the exception werefish. The same remark applies to crocodile and some lizard excrements, which, based on the observations in the Silesian Zoological Garden, left their faeces in the aquatic environment. Only those that left at least part of their faeces in the terrestrial environment were selected for subsequent observations. These were snakes [the king python (*Python regius*), the tiger python (*Python molurus*), the reticulated python (*Malayopython reticulatus*), the common boa (*Boa constrictor*), the king cobra (*Ophiophagus hannah*), the Korean rat snake (*Elaphe anomala*), the common European viper (*Vipera berus*)], lizards [the komodo dragon (*Varanus komodoensis*)], and turtles [the Mediterranean tortoise (*Testudo hermanni*), the steppe tortoise (*Testudo horsfieldii*), the Indian star tortoise (*Geochelone elegans*), the Spanish pond turtle (*Mauremys leprosa*), and the Nile soft shell turtle (*Trionyx triunguis*)].

Authors' contributions

MAS, BJP, TB designed field research. DS, GLG, BJP, MAS, DS, PG, AL provided documentation on fossil material. All authors contributed to writing the paper; all authors edited the final version of manuscript.

Corresponding author

Correspondence to Mariusz A. Salamon

Competing interests

We declare we have no competing interests.

Acknowledgements

We are particularly grateful to Marek Mitrenga, Director of the Silesian Zoological Garden, for making it possible for us to observe the faeces of modern reptiles. Andrzej Malec and Adriana Strzelczyk from the Silesian Zoological Garden provided help, logistic support and information on the mode of life and diet of reptiles kept in the Silesian Zoological Garden. Marek Pastuszek from ZOO Wrocław is acknowledged for providing us with photos of the faeces of extant reptiles. We would also like to thank the dozens of breeders from Poland and the Czech Republic for acquiring modern research material. Our thanks are also due to the management of the Turów Brown Coal Mine for granting permission to enter the plant, and in particular to Ewa Dąbrowska, who supported us with advice and provided all logistical assistance during the field works. Eligiusz Szeląg is acknowledged for providing an access to Olympus BX51 polarizing microscope. This research Project is partially supported by the National Science Centre, Poland (www.ncn.gov.pl), Grant No. 2019/32/C/NZ4/00150 and by the Institute of Geological Sciences, University of Wrocław (subvention no. (501) KD76). GLG acknowledges funding from Forschungskredit of the University of Zurich, Grant no. [FK-20-110].

References

1. Hunt, A. P. & Lucas, S. G. Cenozoic vertebrate trace fossils of North America: ichnofaunas, ichnofacies and biochronology. *New Mexico Museum of Natural History and Science Bulletin* **42**, 17–41 (2007).
2. Dvořák, Z., Mach, K., Prokop, J. & Knor, S. Třetihorni fauna severočeské hnědouhelné pánve, 1–176 (Nakladatelství Granit, 2010).
3. Godfrey, J. S & Smith, B. J. Shark-bitten vertebrate coprolites from the Miocene of Maryland. *Naturwissenschaften* **97**, 461–467 (2010).
4. Pesquero, D. M., Souza-Egipsy, V., Alcalá, L., Ascaso, C. & Fernández-Jalvo, Y. Calcium phosphate preservation of faecal bacterial negative moulds in hyaena coprolites. *Acta Palaeontologica Polonica* **59**, 997–1005 (2014).

5. Dentzien-Dias, P., Carrillo-Briceño, J. D., Francischini, H. & Sánchez, R. Paleoecological and taphonomical aspects of the Late Miocene vertebrate coprolites (Urumaco Formation) of Venezuela. *Palaeogeogr. Palaeoclimatol. Palaeoecol*. **490**, 590–603 (2018).
6. Tomassini, L. R., Montalvo, I. C., Bargo, M. S., Vizcaíno, F. S. & Cuitiño, I. J. Sparassodonta (Metatheria) coprolites from the early-mid Miocene (Santacrucian age) of Patagonia (Argentina) with evidence of exploitation by coprophagous insects. *Palaios* **34**, 639–651 (2019).
7. Farlow, O. J., Chin, K., Argast, A., Poppy, S. Coprolites from the Pipe Creek Sinkhole (Late Neogene, Grant Country, Indiana, U.S.A.). *J. Vertebr. Paleontol*. **30**, 959–969 (2020).
8. Hunt, A. P., Chin, K. & Lockley, M. *The palaeobiology of vertebrate coprolites.* (ed Donovan, S.) 221–240 (Wiley, 1994).
9. Pesquero, D. M., Salesa, J. M., Espílez, E., Mampel, L., Siliceo, G. & Alcalá, L. An exceptionally rich hyaena coprolites concentration in the Late Miocene mammal fossil site of La Roma 2 (Terual, Spain): Taphonomical and palaeoenvironmental inferences. *Palaeogeography, Palaeoclimatology, Palaeoecology* **311**, 30–37 (2011).
10. Amstutz, G. C. Coprolites: a review of the literature and a study of specimens from southern Washington. *Journal of Sedimentary Petrology* **28**, 498–508 (1958).
11. Seilacher, A., Marshall, C., Skinner W. C. & Tsuihiji, T. A fresh look at sideritic "coprolites". *Paleobiology* **27**, 7–13 (2001).
12. Dake, H. C. Northwest gem trails: Portland, Oregon. (Mineralogist Publishing Company, 1939).
13. Dake, H. C. Washington coprolites again. *Mineralogist* **28**, 2–6 (1960).
14. Major, D. Origin of Washington „coprolites". *Mineralogist* **20**, 387–389 (1939).
15. Roberts, A. E. Geology and coal resources of the Toledo-Castle Rock district, Cowlitz and Lewis countries, 1–71 (U.S. Geological Survey Bulletin, 1958).
16. Danner, W. R. Origin of the siderite coprolite-like bodies of the Wilkes Formation, late Miocene, of southwestern Washington. *Canadian Mineralogist*, 571 (1968).
17. Danner, W. R. The pseudocoprolites of Salmon Creek, Washington. (University of British Columbia Department of Geological Sciences Report, 1994).
18. Danner, W. R. The pseudocoprolites of Salmon Creek, Washington. (British Columbia Paleontological Symposium, 1997).

19. Love, J. D. & Boyd D. W. Pseudocoprolites in the Mowry Shale (Upper Cretaceous), northwest Wyoming. *University of Wyoming Contribution to Geology* **28**, 139–144 (1991).
20. Spencer, P. K. & Tuttle, F. H. Coprolites or pseudo-coprolites? New evidence concerning the origin of Washington coprolites. *Geological Society of America* **12**, 153 (1980).
21. Spencer, P. K. The „coprolites" that arent: The straight poop on specimens from the Miocene of southwestern Washington State, Ichnos. *An International Journal for Plant and Animal Traces* **2**, 231–236 (1993).
22. Spencer, P. K. The method of multiple working hypotheses in undergraduate education with an example of its application and misapplication. *Journal of Geoscience Education* **45**, 123–128 (1997).
23. Hardie, J. K. Dolomite and siliciclastic dikes and sills in marginal-marine Cretaceous coals of central Utah. 1– 19 (U.S. Geological Survey Bulletin 2087, 1994).
24. Mustoe, E. G. Enigmatic origin of ferruginous „coprolites": Evidence form the Miocene Wilkes Formation, southwestern Washington. *GSA Bulletin* **113**, 673–681 (2001).
25. Piątkowska, A., Kasiński, J. & Graniczny, M. Analysis of integrated remote sensing and tectonic data in the Żytawa-Zgorzelec Depression (SW Poland). *Przegląd Geologiczny* **48**, 991–999 (2000).
26. Jęczmyk, M. & Sztromwasser, E. Kominowe syderytowe dajki karbonatytowe w bazaltoidach Kopalni Węgla Brunatnego Turów (Sudety). *Przegląd Geologiczny* **46**, 87–94 (1998).
27. Kasiński J. R. Atlas geologiczny trzeciorzędowej asocjacji brunatnowęglowej w polskiej części Niecki Żytawskiej. Skala 1:50 000 (PIG, 2000).
28. Kasiński, J. R., Badura, J., Pańczyk, M., Pécskay, Z., Saternus, A., Słodkowska, B. & Urbański, P. Osady paleogeńskie w polskiej części niecki żytawskiej – nowe światło na problem wieku zapadliska tektonicznego. *Biuletyn Państwowego Instytutu Geologicznego* **461**, 295–324 (2015).
29. Marcinkowski, B. Przejawy mineralizacji kruszcowej w kompleksie magmowo-metamorficznym okolic Bogatyni. *Kwartalnik Geologiczny* **29**, 551–570 (1985).
30. Szynkiewicz A. *Wiek utworów neogenu w zachodniej części Dolnego Śląska*. (eds Żelażniewicz A., Wojewoda J. & Ciężkowski W.) 11–18 (WIND, 2011).

31. Kasiński, J. R., Badura, J. & Przybylski, B. *Cenozoic depressions at the northwestern Sudetic Foreland*. (eds Ciężkowski, A., Wojewoda, J. & Żelaźniewicz, A.) 183–196 (WIND, 2003).
32. Kasiński, J. R., Piwocki, M., Swadowska, E. & Ziembińska-Tworzydło, M. Lignite of the Polish Lowlands Miocene: Characteristics on a base of selected profiles. *Biuletyn Państwowego Instytutu Geologicznego* **439**, 99–154 (2010).
33. Kasiński, J. R. & Wiśniewski, J. *Stanowisko 5. Formacja biedrzychowska*. (eds Ciężkowski, A., Wojewoda, J. & Żelaźniewicz, A.) 31–33 (WIND, 2003).
34. Sadowska, A. *Palynostratigraphy and paleoecology Neogene of the Sudetic Foreland*. (eds Cwojdziński, S., Dyjor, S., Staśko, S. & Żelaźniewicz, A.) 37–47 (Annales Soc. Geolog. Polon., special volume, 1995).
35. Durska, E. A 90 m-thick coal seam In the Lubstów lignite deposit (Central Poland) palynological analysis and sedimentary environment. *Geological Quarterly* **52**, 281–290 (2008).
36. Paszcza, K. Nowe znaleziska polskich tektytów z obszaru niecki żytawskiej. *Przegląd Geologiczny* **69**, 244–247 (2021).
37. Reinach, A. von. Schildkrötenreste im Mainzer Tertiärbecken und in benachbarten ungefähr gleichaltrigen. *Abhandlungen der Senckenbergischen Naturforschenden Gesellschaft* **28**, 1–135 (1900).
38. Młynarski, M. & Roček, Z. Chelonians (Reptilia, Testudines) from the Lower Miocene locality Dolnice (Bohemia, Czechoslovakia). *Časopis pro mineralogii a geologii* **30**, 397–408 (1985).
39. Laube, G. C. Synopsis der Wirbelthierfauna derBöhm. Braunkohlenformation. *Abhandlungen desdeutschen naturwissenschaftlich-medicinischen Verei-nes für Böhmen "Lotos"* **2**, 107–186 (1901).
40. Obrhelová, N. Über einen Serranid (Pisces) ausdem nordböhmischen Süßwassertertiär. *Časopis promineralogii a geologii* **16**, 371–387 (1971).
41. Špinar, Z. V. Tertiary frogs from Central Europe, 1–286 (Academy of Science, 1972).
42. Obrhelová, N. & Obrhel, J. Paläoichthyologie und Paläoökologie des kontinentalen Tertiärs und Quartärsin der ČSSR. *Zeitschrift für geologische Wissenschaften* **15**, 709–731 (1987).
43. Szyndlar, Z. Oligocene snakes of southern Germany. *Journal of Vertebrate Paleontology* **14**, 24–37 (1994).

44. Böhme, M. Revision der oligozänen und unter-miozänen Vertreter der Gattung *Palaeoleuciscus* (Teleostei, Cyprinidae) Mitteleuropas, 1–109 (University Leipzig, 1996).
45. Böhme, M. *Archaeotriton basalticus* (v. Meyer, 1859) (Urodela, Salamandridae) aus dem Unteroligozänvon Hammerunterwiesenthal (Freistaat Sachsen). *Abhandlungen des Staatlichen Museums für Mineralogieund Geologie zu Dresden* **43/44**, 265–280 (1998).
46. Böhme, M. Revision of the cyprinids from the Early Oligocene of the České Středohoří Mountains, and the phylogenetic relations-hips of Protothymallus Laube 1901 (Teleostei, Cyprinidae, Gobioninae). *Acta Mus. Nat. Pragae, Ser. B, Hist. Nat*. **63**, 175–194 (2007).
47. Gaudant, J. Rectifications de nomenclature relatives à l'ichthyofaune oligo-miocène dulcaquicoles de Bohême. *Journal of the Czech Geological Society*, **41**: 91–96 (1996).
48. Gaudant, J. Cinq nouveaux gisements de Pelobatidae (Amphibiens anoures) dans l'Oligocène d'Europe centrale. *Neues Jahrbuch für Geologie und Paläontologie, Monatshefte* **1997**, 434–446 (1997).
49. Micklich, N. & Böhme, M. Wolfsbarsch-Funde (Perciformes, Moronidae) aus den Süßwasser-Diato-miten von Kučlín (Böhmen) nebst Anmerkungen zurtaxonomischen Stellung von *"Perca" lepidota* aus den Süßwasserkalken von Öhningen (Baden). *Paläontologische Zeitschrift* **71**, 117–128 (1997).
50. Bellon, H., Bůžek, C., Gaudant, J., Kvaček, Z. & Walther, H. The České Středohoří magmatic complex inNorthern Bohemia 40K-40Ar ages for volcanism andbiostratigraphy of the Cenozoic freshwater formations. *Newsletters on Stratigraphy* **36**, 77–103 (1998).
51. Kvaček, Z. & Walther, H. Reconstruction of vegetation and landscape development uring volcanic activity in the České Středohoří Mountains. *Geolines* **15**, 60–64 (2003).
52. Mikuláš, R., Fejfar, O., Ulrych, J., Žigová, A., Kadlecová, E. & Cajz, V. A study of the Dětaň locality (Oligocene, Doupovské hory Mts. Volcanic Complex, Czech Republic): collection of field data and starting points for interpretation. *Geolines* **15**, 91–97 (2003).
53. Fejfar, O. & Kaiser, T. Insect bone-modification and paleoecology of Oligocene mammal-bearing sites in the Doupov Mountains, Northern Bohemia. *Palaeontologia Electronica* **8**, 8A, 11p (2005).

54. Čerňanský, A. & Augé, M. Additions to the lizard fauna (Squamata: Lacertilia) of the Upper Oligocene (MP 28) of Herrlingen 8, Southern Germany. *Neues Jahrbuch für Geologie und Paläontologie - Abhandlungen* **264/1**, 11–19 (2012).
55. Čerňanský, A. & Augé, M. New species of the genus *Plesiolacerta* (Squamata: Lacertidae) from the upper Oligocene (MP 28) of southern Germany and a revision of the type species *Plesiolacerta lydekkeri*. *Palaeontology* **56**, 79–94 (2013).
56. Čerňanský, A., Klembara, J. & Müller, J. The new rare record of the late Oligocene lizardsand amphisbaenians from Germany and its impacton our knowledge of the European terminal Palaeogene. *Palaeobiodiversity and Palaeoenvironments* **96**, 559–587 (2016).
57. Georgalis, G. L. & Joyce, W. G. A review of the fossil record of Old World turtles of the clade *Pan-Trionychidae*. *Bulletin of the Peabody Museum of Natural History* **58**, 115–208 (2017).
58. Ivanov, M. The oldest known Miocene snake fauna from Central Europe: Merkur-North locality, Czech Republic. *Acta Palaeontologica Polonica* **47**, 513–534 (2002).
59. Klembara, J. Beitrag zur Kenntnis der Subfamilie Anguinae (Reptilia, Anguidae). *Acta UniversitatisCarolinae, Geologica* **2**, 121–168 (1981).
60. Klembara, J. A new anguimorph lizard from the Lower Miocene of North-West Bohemia, Czech Republic. *Palaeontology* **51**, 81–94 (2008).
61. Klembara, J. A new species of *Pseudopus* (Squamata, Anguidae) from the early Miocene of Northwest Bohemia (Czech Republic). *Journal of Vertebrate Paleontology* **32**, 854–866 (2012).
62. Klembara, J. New finds of anguines (Squamata, Anguidae) from the Early Miocene of North-West Bohemia (Czech Republic). *Paläontologische Zeitschrift* **89**, 171–195 (2015).
63. Čerňanský, A. & Joniak, P. Nové nálezy jašteríc (Sauria, Lacertidae) z neogénnych sedimentov Slovenskaa Českej republiky. *Acta Geologica Slovaca* **1**, 57–64 (2009).
64. Čerňanský, A. & Bauer, A. M. *Euleptes gallica* Müller (Squamata: Gekkota: Sphaerodactylidae) from the Lower Miocene of North-West Bohemia, Czech Republic. *Folia Zoologica* **59**, 323–328 (2010).
65. Čerňanský, A. A revision of chamaeleonids from the Lower Miocene of the Czech Republic with description of a new species of *Chamaeleo* (Squamata, Chamaeleonidae). *Geobios* **43**, 605–613 (2010).

650 66. Čerňanský, A. The oldest known European Neogene girdled lizard fauna (Squamata,
651 Cordylidae), with comments on Early Miocene immigration of African taxa.
652 *Geodiversitas* **34**, 837–848 (2012).
653 67. Čerňanský, A., Rage, J-C. & Klembara, J. The Early Miocene squamates of
654 Amöneburg (Germany): the first stages of modern squamates in Europe. *Journal of*
655 *Systematic Palaeontology* **13**, 97–128 (2015).
656 68. Joyce, W. G. A review of the fossil record of turtles of the clade *Pan-Chelydridae*.
657 *Bulletin of the Peabody Museum of Natural History* **57**, 21–56 (2016).
658 69. Klembara, J. & M. Rummel. New material of *Ophisaurus*, *Anguis* and *Pseudopus*
659 (Squamata, Anguidae, Anguinae) from the Miocene of the Czech Republicand
660 Germany and systematic revision and palaeobiogeography of the Cenozoic Anguinae.
661 *Geological Magazine* **155**, 20–44 (2018).
662 70. Chroust, M., Mazuch, M., Ivanov, M., Ekrt, B. & Luján, À. H. First remains of
663 *Diplocynodon* cf. *ratelii* fromthe early Miocene sites of Ahníkov (Most Basin, Czech
664 Republic). *Bulletin of Geosciences* **96**, 123–138 (2021).
665 71. Hanesch, M. Raman spectroscopy of iron oxides and (oxy) hydroxides at low laser
666 power and possible applications in environmental magnetic studies. *Geophys. J. Int.*
667 **177**, 941–948 (2009).
668 72. Rutt, H. N. & Nicola, J. H. Raman spectra of carbonates of calcite structure. *J. Phys.*
669 *C: Solid State Phys.* **7**, 4522–4528 (1974).
670 73. Goldhaberet, M. G., Reynolds, L. R. & Rye, O. R. Relationship of modern
671 groundwater chemistry to the origin and reduction of south Texas roll-front uranium
672 deposits, 1–220 (U.S. Geological Survey Professional Paper, 1979).
673 74. Harris, R. & King, K. J. *Geological classification and origin of radioactive*
674 *mineralization in Wyoming*. (eds Snoke, A. W., Steidmann, J. R. & Roberts, S. M.)
675 898-916 (Geological Survey of Wyoming Memoir, 1993).
676 75. Chin, K. & Kirkland, J. I. Probable herbivore coprolites from the Upper Jurassic
677 Mygatt-Moore Quarry, Western Colorado. *Mod. Geol*. **23**, 249–275 (1998).
678 76. Fiorelli, L. E., Ezcurra, M. D., Hechenleitner, E. M., Argañaraz, E., Taborda, J. R. A.,
679 Trotteyn, M. J., Belén von Baczko, M. & Desojo, J. B. The oldest known communal
680 latrines prove evidence of gregarism in Triassic megaherbivores. *Scientific Reports* **3**,
681 3348 (2013).
682 77. Bajdek, P., Qvarnström, M., Owocki, K., Sulej, T., Sennikov, A. G., Golubev, V. K. &
683 Niedźwiecki, G. Microbiota and food residues including possible evidence of pre-

mammalian hair in Upper Permian coprolites from Russia. *Lethaia* **49**, 455–477 (2016).

78. Mayer, W. V. The hair of California mammals with keys to the dorsal guard hairs of California mammals. *American Midland Naturalist* **48**, 480–512 (1952).
79. Kshirsagar, S. V., Singh, B. Fulari, S. P. Comparative study of human and animal hair in relation with diameter and medullary index. *Indian Journal of Forensic Medicine and Pathology* **2**, 105–108 (2009).
80. Taru P. & Backwell L. Identification of fossil hairs in Parahyaena brunnea coprolites from Middle Pleistocene deposits at Gladysvale cave, South Africa. *Journal of Archaeological Science* 40, 3674–3685 (2013).
81. Wegner, R. N. Tertiär und umgelagerte Kreide bei Oppeln (Oberschlesien). *Palaeontographica* **60**, 3–4 (1913).
82. Georgalis, G. L. & Smith, K. T. Constrictores Oppel, 1811 – the available name for the taxonomic group uniting boas and pythons. *Vertebrate Zoology* **70**, 291–304 (2020).
83. Pope, R., Helmstetter, C., Lignot, J. H. & Secor, S. Bone absorption through specialised intestinal cells in juvenile Burmese pythons. Comp. *Biochem Physiol*. **146A**, S174 (2007).
84. Nørgaard, S., Andreassen, K., Lind Malte, C., Enok S. & Wang, T. Low cost of gastric acid secretion during digestion in ball pythons. *Comparative Biochemistry and Physiology Part A: Molecular & Integrative Physiology* **194**, 62–66 (2016).

Captions to figures:

Fig. 1. A. Map of central Europe with mentioned in the text areas marked as red rectangles. **B.** Geology of Zittau Basin. **C.** Synthetic lithostratigraphic section of Paleogene and Neogene sediments of the Polish part of the Zittau Basin (slightly modified after [36]).

Fig. 2. Miocene turtle and snake coprolites from the Turów lignite mine, Poland **(A, B, E-G)**, compared with modern turtle and snake excrements **(C, D, H-M)** and fossil remain from the Turów lignite mine, Poland **(N)**. Scale bar equals 10 mm. **A, B.** coprolites, morphotype M1. **C, D.** modern excrements of *Testudo horsfieldii* (C), and *Testudo hermanni* (D). **E-G.** coprolites, morphotype M2. **H, I.** modern excrements of *Python regius*. **J.** modern excrement of *Boa constrictor*. **K.** modern excrement of *Ophiophagus hannah*. **L.** modern excrement of *Elaphe anomala*. **M.** modern excrement of *Vipera berus*. **N**. Shell fragment of Testudinoidea indet. from the Turów lignite mine, Poland **(N)**.
Red arrows in A and B = coalified inclusions, yellow arrows in F and G = fine striations.

Fig. 3. Hair-like structure identified in coprolites (morphotype 2). A-C. Optical microscopy. D-H. SEM images. F, G. Magnification of scale-like pattern. H. Magnification of internal hair-like cellular structure (above the dotted line) and highly porous surrounding matrix (below dotted line).

Fig. 4. (A-F) BSE image of the coprolite matrix with preserved structures. The red frame indicates the area of the Raman image from Fig. 5. **(A1-F1)** topographic pictures of the area from the A-F images. **(G, H)** BSE image of multi-layered iron oxides form with siderite center. **(I, J)** BSE image of the non-porous type of coprolite matrix. Mineral abbreviations: Gth - goethite, Hem - hematite, Sd - siderite.

Fig. 5. Raman spectrum of **(A)** hematite, **(B)** goethite, **(C)** siderite from coprolite matrix.

Fig. 6. The difference in the fluorescence level in the Raman spectrum of hematite from the structures. **(A)** Reflected light image of the elongated structure. **(B)** Cluster analysis of the structure and matrix Raman mapping. **(C)** Raman spectrum of hematite from structure area (1) and coprolite matrix (2).

Figures

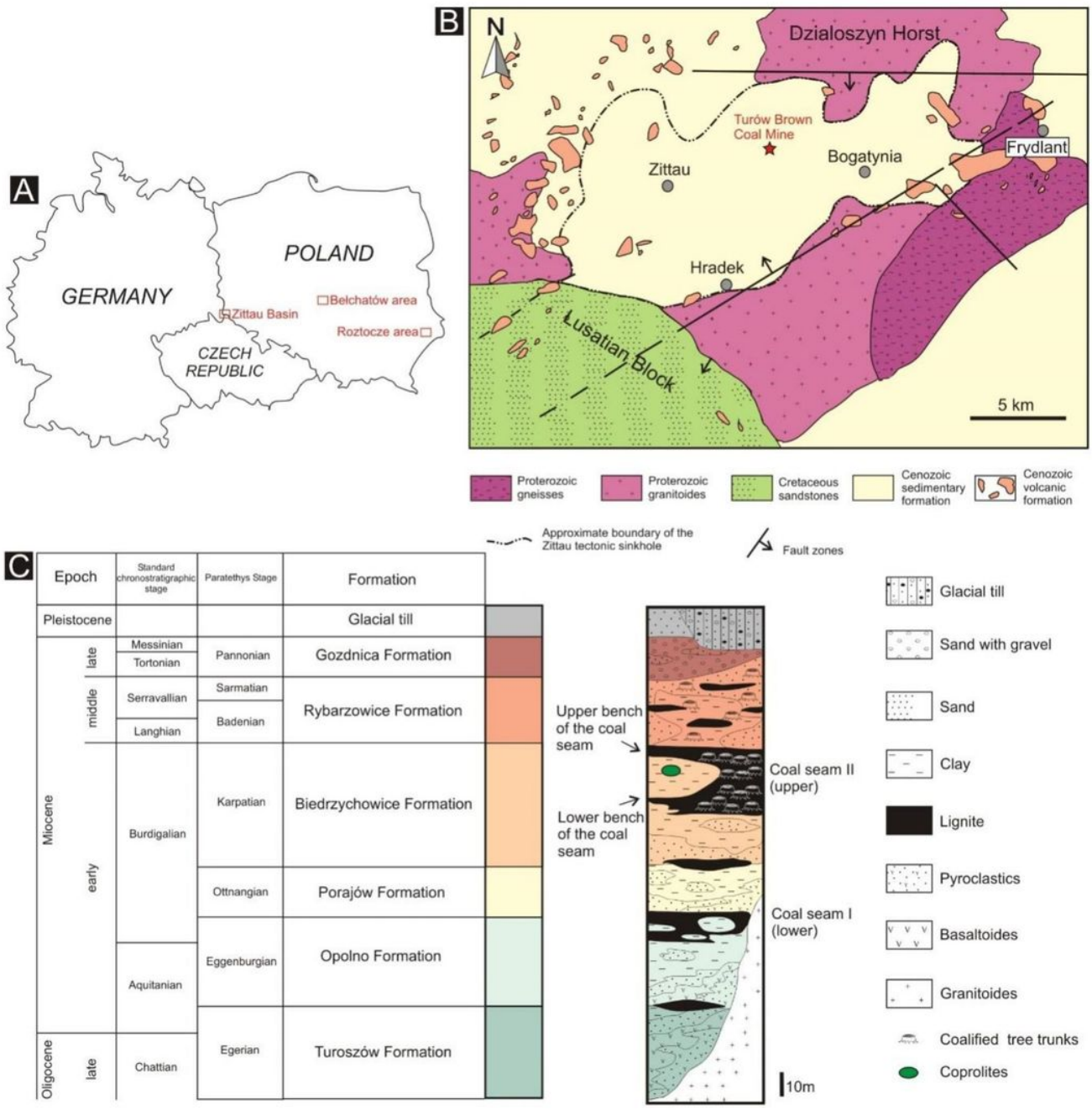

Figure 1

A. Map of central Europe with mentioned in the text areas marked as red rectangles. B. Geology of Zittau Basin. C. Synthetic lithostratigraphic section of Paleogene and Neogene sediments of the Polish part of the Zittau Basin (slightly modified after 36).

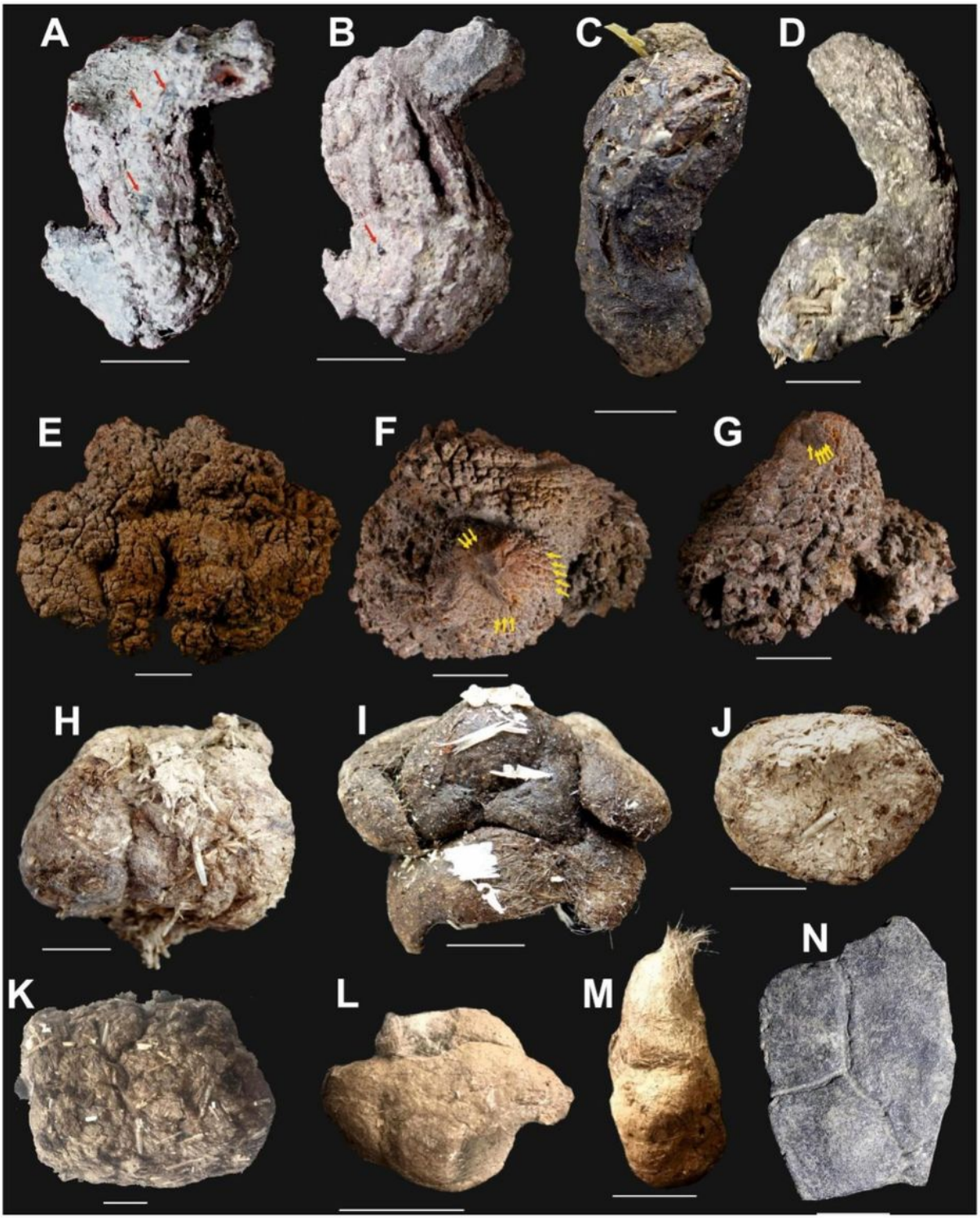

Figure 2

Miocene turtle and snake coprolites from the Turów lignite mine, Poland (A, B, E-G), compared with modern turtle and snake excrements (C, D, H-M) and fossil remain from the Turów lignite mine, Poland (N). Scale bar equals 10 mm. A, B. coprolites, morphotype M1. C, D. modern excrements of Testudo horsfieldii (C), and Testudo hermanni (D). E-G. coprolites, morphotype M2. H, I. modern excrements of Python regius. J. modern excrement of Boa constrictor. K. modern excrement of Ophiophagus hannah. L.

modern excrement of Elaphe anomala. M. modern excrement of Vipera berus. N. Shell fragment of Testudinoidea indet. from the Turów lignite mine, Poland (N). Red arrows in A and B = coalified inclusions, yellow arrows in F and G = fine striations

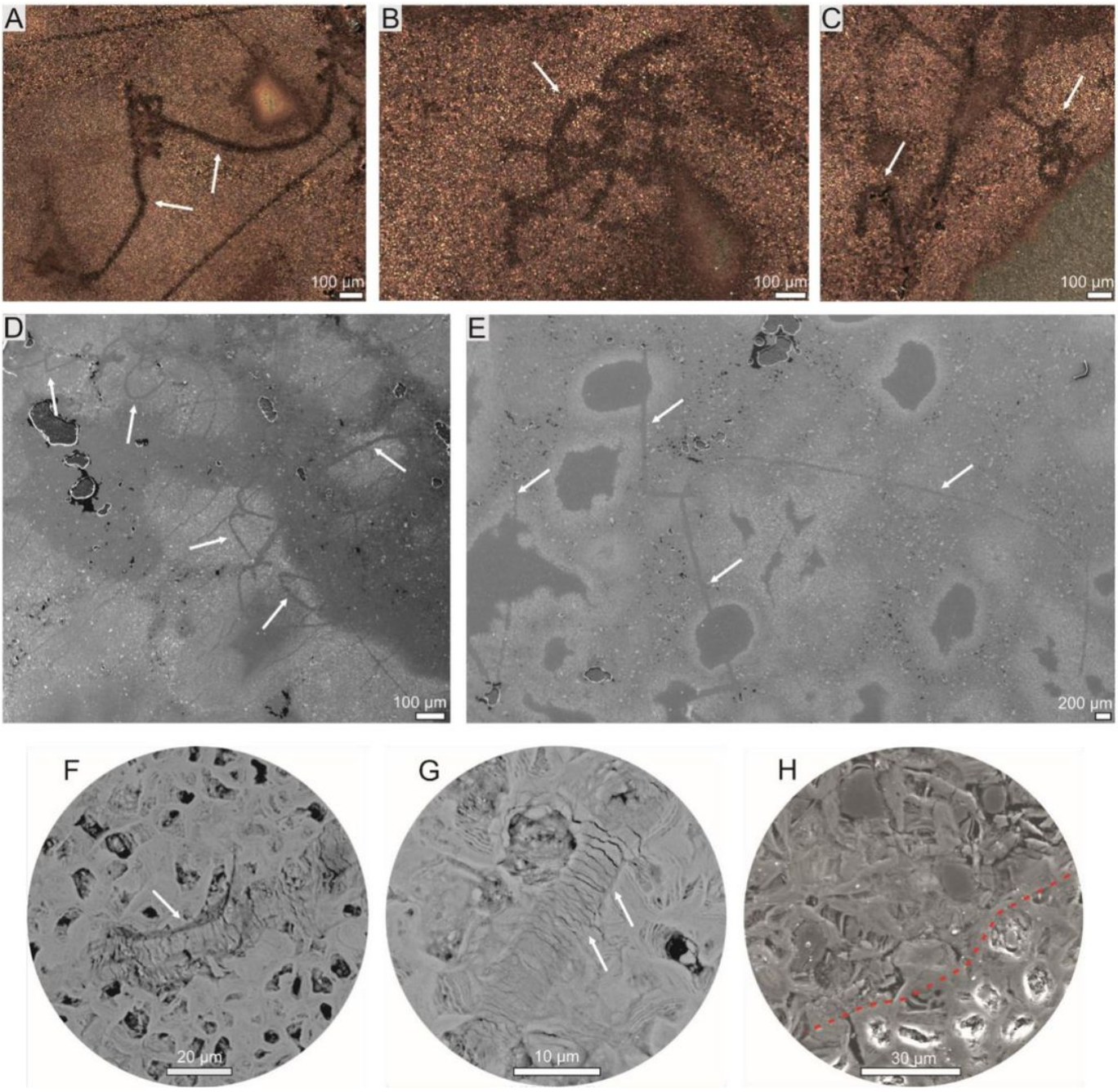

Figure 3

Hair-like structure identified in coprolites (morphotype 2). A-C. Optical microscopy. D-H. SEM images. F, G. Magnification of scale-like pattern. H. Magnification of internal hair-like cellular structure (above the dotted line) and highly porous surrounding matrix (below dotted line).

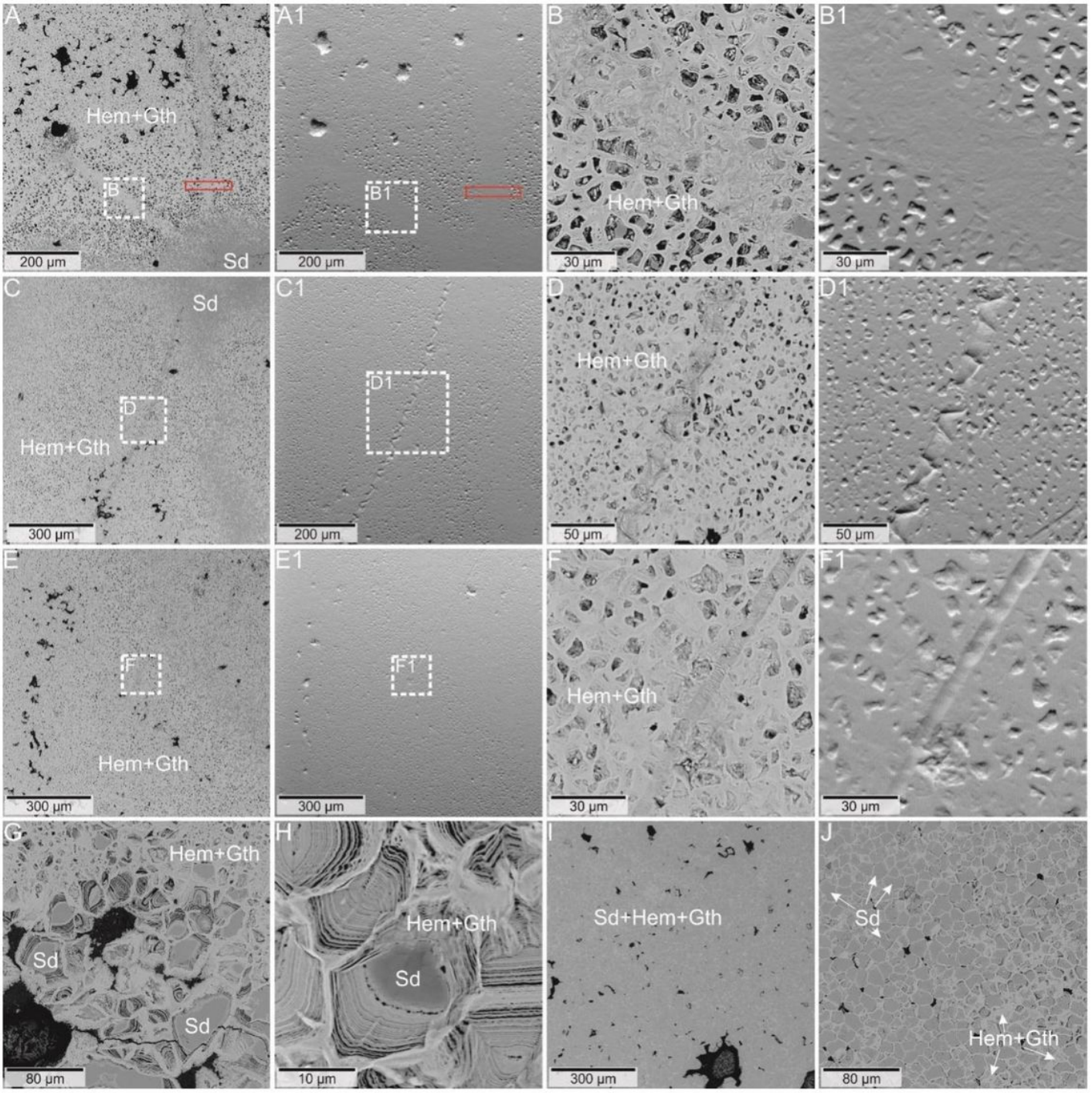

Figure 4

(A-F) BSE image of the coprolite matrix with preserved structures. The red frame indicates the area of the Raman image from Fig. 5. (A1-F1) topographic pictures of the area from the A-F images. (G,H) BSE image of multi-layered iron oxides form with siderite center. (I,J) BSE image of the non-porous type of coprolite matrix. Mineral abbreviations: Gth - goethite, Hem - hematite, Sd - siderite.

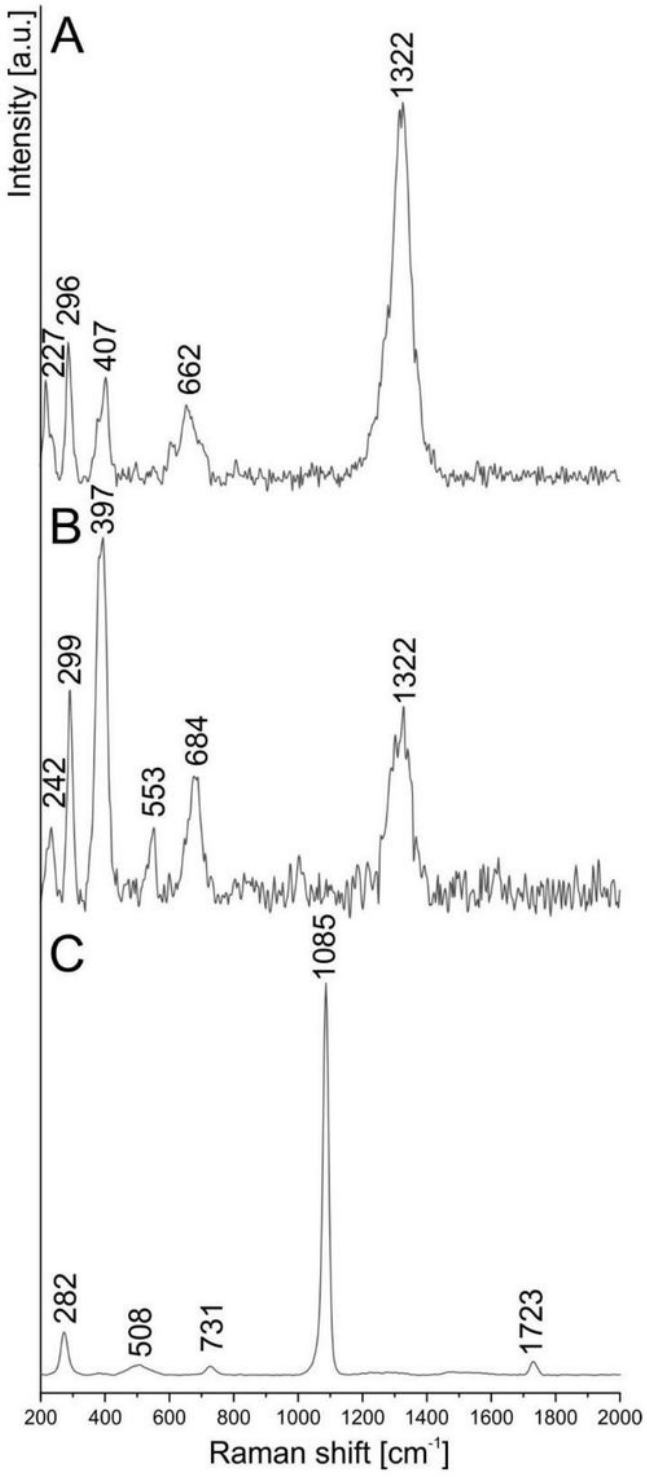

Figure 5

Raman spectrum of (A) hematite, (B) goethite, (C) siderite from coprolite matrix.

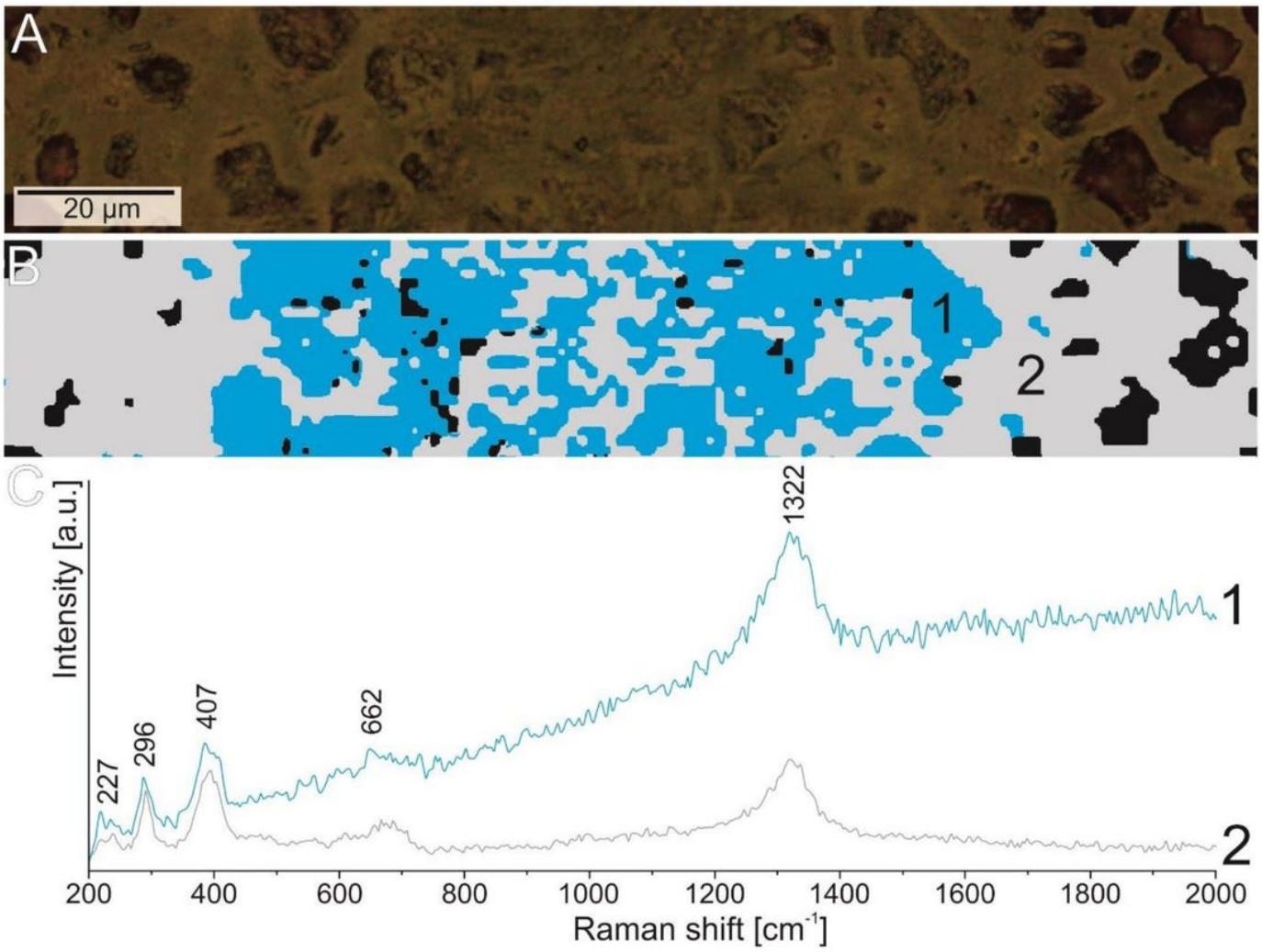

Figure 6

The difference in the fluorescence level in the Raman spectrum of hematite from the structures. (A) Reflected light image of the elongated structure. (B) Cluster analysis of the structure and matrix Raman mapping. (C) Raman spectrum of hematite from structure area (1) and coprolite matrix (2)

Supplementary Files

This is a list of supplementary files associated with this preprint. Click to download.

- Supplementarymovie01.avi
- Supplements.docx